The First Takeoff of a Biologically Inspired At-Scale Robotic Insect

Robert J. Wood, *Member, IEEE*

***Abstract*—Biology is a useful tool when applied to engineering challenges that have been solved in nature. Here, the emulous goal of creating an insect-sized, *truly micro* air vehicle is addressed by first exploring biological principles. These principles give insights on how to generate sufficient thrust to sustain flight for centimeter-scale vehicles. Here, it is shown how novel manufacturing paradigms enable the creation of the mechanical and aeromechanical subsystems of a microrobotic device that is capable of Diptera-like wing trajectories. The results are a unique microrobot: a 60 mg robotic insect that can produce sufficient thrust to accelerate vertically. Although still externally powered, this micromechanical device represents significant progress toward the creation of autonomous insect-sized micro air vehicles.**

***Index Terms*—Actuators, aerial robotics, biologically inspired robotics, microrobotics.**

I. Introduction

THE STUDY of flight began with mankind's awe and envy of flying organisms. Regarding nature's smallest fliers, contemporary studies have given detailed insights into the remarkable maneuverability of some flying insects. Insects encompass the most agile flying objects on earth, including all things man-made and biological. Until recently, the aerodynamic mechanisms by which insects achieve this performance were not understood in the framework of classical aerodynamic theory. Now, through the work of Ellington *et al*. [1], [2], Dickinson *et al*. [3]–[5], and others, the complex aerodynamics of a periodic wing stroke at low Reynolds numbers (less than 1000) is understood well enough to be used as a design tool for engineers that wish to recreate these devices.

But, this understanding is not sufficient to create effective robotic insects. Novel manufacturing paradigms must be considered concurrently in order to achieve the level of efficiency and durability that millimeter-scale flying machines will require. The high speed, highly articulated mechanisms that are necessary to reproduce insect-like wing motions exist on a scale that is between microelectromechanical systems (MEMS) [6] and "macro" devices [7]. Thus, a "meso" scale rapid fabrication method, called smart composite microstructures (SCMs), is used to bridge this gap (for details, see [8]). Previous research has yielded concise design rules for the development of flexure-based micromechanical structures based upon the SCM process [9], [10]. These design rules form the basis for the device that is described here: an insect-sized flapping-wing micro air vehicle (MAV).

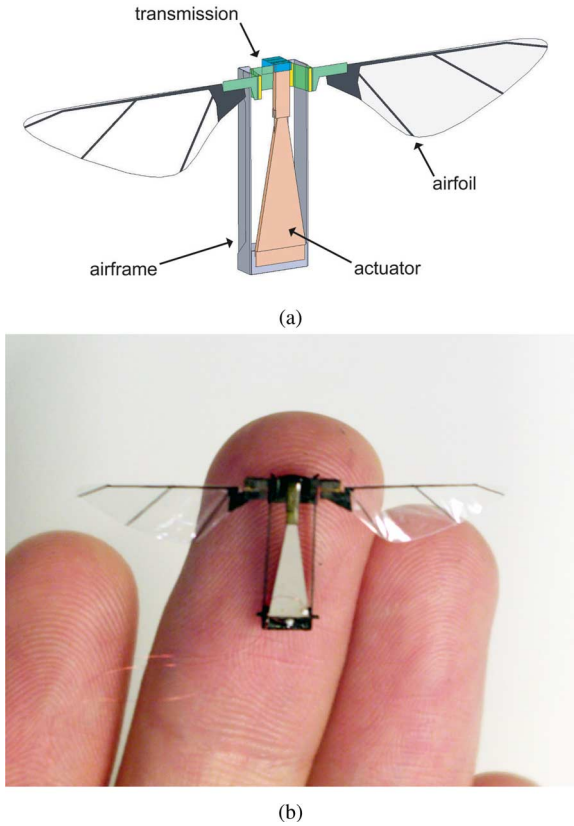

Fig. 1. (a) Conceptual drawing highlighting the four primary mechanical and aeromechanical components. (b) First insect-scale flying robot able to takeoff.

Insect-like vehicles have vast potential applications including search and rescue, hazardous environment exploration, surveillance, reconnaissance, and planetary exploration [11]. The prototype robotic insect is shown in Fig. 1 (for more details, see http://micro.seas.harvard.edu).

II. Insect Flight

Insects of the order Diptera generate aerodynamic forces with a three degree-of-freedom wing trajectory that consists of a large wing stroke (that defines the stroke plane), pronation and supination (collectively called wing rotation) about a longitudinal wing axis, and stroke plane deviation [12]–[15]. This discussion will not consider stroke plane deviation: for some hovering Dipteran insects that have a nearly horizontal stroke plane, it does not appear that stroke plane deviation plays a significant role in lift

Manuscript received July 23, 2007; revised October 21, 2007. This paper was recommended for publication by Associate Editor D. Sun and Editor F. Park upon evaluation of the reviewers' comments.

The author is with the School of Engineering and Applied Sciences, Harvard University, Cambridge, MA 02139 USA (e-mail: rjwood@seas.harvard.edu).

Color versions of one or more of the figures in this paper are available online at http://ieeexplore.ieee.org.

Digital Object Identifier 10.1109/TRO.2008.916997

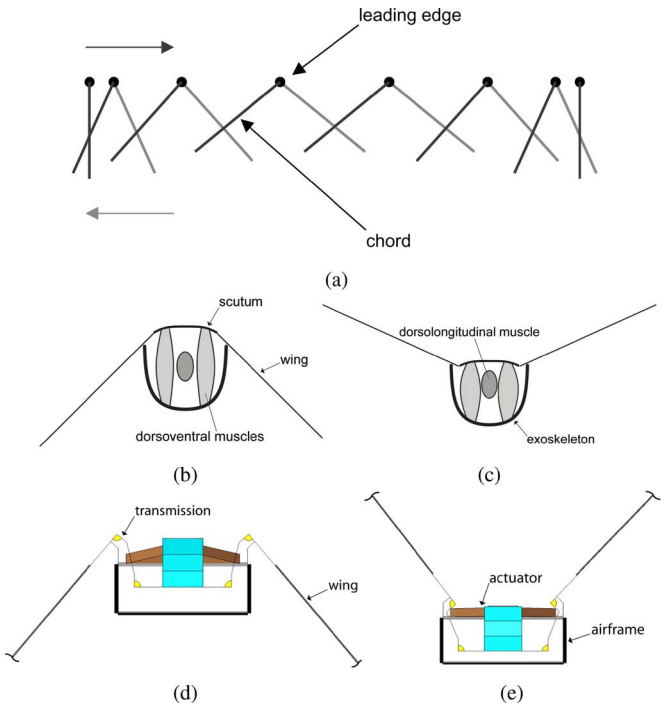

Fig. 2. Approximate wing motion (a) projected onto a 2-D plane (ignoring stroke plane deviation) along with a diagram of a Dipteran insect thorax showing generation of downstroke (b) and upstroke (c) (adapted from [17]). For comparison, the anterior diagram of the robotic thorax motion is also shown. The wing moves from the lower extreme (d) to the upper (e) by linear actuator motions coupled through a flexure-based transmission.

generation [3]. This considerably simplifies the analysis of the wing trajectory and the construction of the transmission mechanism. The desired two degree-of-freedom trajectory profile is shown in Fig. 2(a). Dipteran insects generate wing motions using indirect flight muscles that pull on a deformable section of the exoskeleton called the scutum [16]. The wing is connected to the pleural wing process at the interface of the scutum and the exoskeleton. Contractions of the dorsoventral muscles depress the scutum and create the upstroke. Contractions of the dorsolongitudinal muscles shorten the thorax and return the scutum to its initial position, generating the downstroke [see Fig. 2(b) and (c)]. Wing rotation is accomplished by smaller muscles (basalar and subalar) that directly apply a torque to the sclerites connected to the wing hinge [17]. While there has been some debate over the concise mechanisms involved in Dipteran thoracic mechanics, there are a few clear characteristics of the wing drive system.

1) Insects utilize a mechanical advantage to amplify the wing stroke.
2) Diptera operate their wing strokes at the natural frequency of the aeromechanical system [13].
3) Some aspects of Dipteran wing trajectories are mechanically "hard-coded" into their morphologies while others are tunable.

Here, we utilize each of these aspects with the creation of a resonant wing-drive system that is mechanically "preprogrammed" with a desired baseline trajectory. A parallel is shown in Fig. 2(b)–(e) between Dipteran thoracic morphology (oversimplified) and the robotic version.

III. Creation of a Robotic Insect

Insect wing trajectories are the basis for the Harvard Microrobotic Fly. If a robotic device can reproduce the necessary aspects of Dipteran wing motion with a similar wing-beat frequency and mass comparable to actual flies, it should be capable of producing sufficient thrust to fly. This device has four primary mechanical components: the airframe (exoskeleton), actuator (flight muscle), transmission (thorax), and airfoils, as is shown in Fig. 1(a). The function of each are simple: 1) the airframe provides a solid ground to the actuator and transmission while contributing minimal mass; 2) the actuator should provide motion with maximal power density; 3) the transmission must efficiently impedance-match the actuator to the load; and 4) the airfoils must remain rigid to hold shape under large aerodynamic loads. The subtleties of these components are described later.

A. Actuation

There is one primary actuator that drives the thorax in a similar configuration to Dipteran dorsoventral muscles, but with bidirectional force. The actuator chosen for this application is a bimorph piezoelectric clamped-free bending cantilever that is optimized for mechanical power delivery and created using SCM [18]. These actuators are chosen because of favorable scalability (compared, for example, to electromagnetic motors) and compatibility with the SCM process. Compared to other actuation technologies, piezoelectric actuators typically have high operating stresses and frequencies. However, piezoceramic materials are dense and brittle and typically achieve relatively small strains (hence the need for mechanical amplification). The ultimate quantity of interest for a hover-capable MAV is the power density (at the frequency of interest). For the sake of a performance metric, biological estimates place the body-mass-specific power density for flying insects between 29 W/kg [19] and 40 W/kg [20] and between 80 W/kg [21] and 83 W/kg [22] for the muscles alone. For comparison, the class of actuators used here have demonstrated power densities of 400 W/kg [23]. This is the first example of where a subsystem of the microrobotic fly exceeds the performance of its biological counterpart.

The design of the actuator is based upon a laminate plate theory model that describes the stress distribution across a multilayered composite structure (see [18] for details of this model). Since the individual layers are thin, the model is simplified to a reduced-tensor notation. However, all desired characteristics of the actuator are included (e.g., displacement, peak force, bandwidth, etc.). The actuators are created with the SCM process: first, individual lamina [$PbZrTiO_3$ (PZT)-5H and M60J carbon fiber/cyanate ester resin prepreg] are laser-micromachined into desired planform shapes. These layers [see Fig. 3(a)] are then stacked and aligned and put through a controlled cure cycle that regulates temperature, pressure, and time of cure. The resulting actuator is fixed to the airframe proximally and the input to the transmission distally. Application of an electric field creates a bending moment in the actuator that deflects the transmission

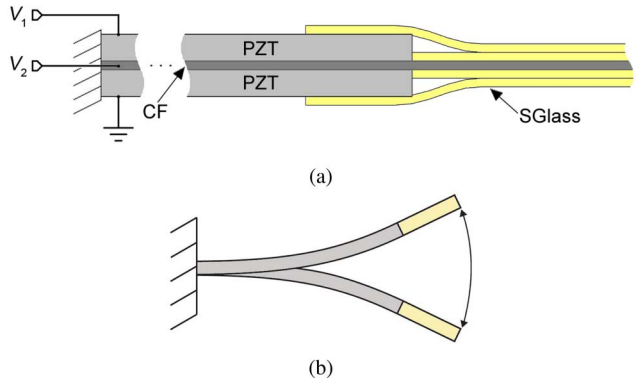

Fig. 3. Overview of the flight muscles used for the Harvard Microrobotic fly. (a) Clamped-free bending cantilever that consists of symmetric layers of laser-micromachined piezoceramic $PbZrTiO_3$ (PZT). (b) Actuator bends (shown exaggerated) as an electric field is applied to either plate.

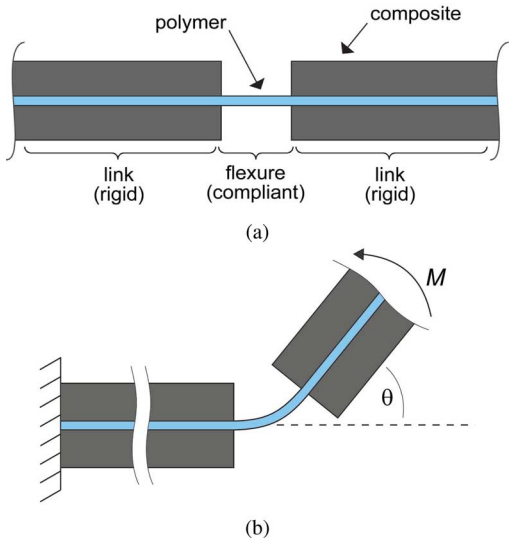

Fig. 4. Cross section of a typical flexure joint used in the thorax of the Harvard Microrobotic Fly. (a) Laser-micromachined carbon fiber reinforced composite face sheets sandwich a thin layer of polyimide. (b) Compliance of the joint is determined by the geometry and material properties such that a moment, M, results in an angular deflection, θ.

[exaggerated in Fig. 3(b)]. These actuators are 40 mg, 12 mm long, and achieve a deflection of greater than ± 400 μm with a bandwidth greater than 1 kHz.

B. Transmission

Similar to the insect model shown in Fig. 2(b) and (c), the transmission amplifies the actuator motion from a translational input to a rotational output. This is done while impedance-matching the load to the actuator: the system is driven at its fundamental resonance, and thus, the dynamics during normal operation are dominated by the wing loading and the actuator losses. Therefore, for efficient electromechanical transduction, it is imperative that the wing loading (as seen by the actuator) is matched to the internal losses of the actuator.

At larger scales, such a device could be assembled with gears and slider mechanisms [24]. However, due to unfavorable surface area scaling, such components would result in significant friction losses as the characteristic size is decreased. Instead, flexures are used in place of revolute joints [25] (see Fig. 4). The desired stroke amplitude is $\pm 60^\circ$; thus, for actuator motion of approximately ± 400 μm, we require a transmission that has a nominal amplification of approximately 2600 rad/m. This is called the *transmission ratio* and is directly analogous to a gear ratio for these compliant mechanisms. Note that this assumes a perfectly compliant transmission. If the stiffness of the transmission is nonzero, the transmission ratio will need to be increased.

There has been significant research into the creation and characterization of flexure-based micromechanical devices [26], and these design rules provide the basis for the creation of the transmission. These flexure mechanisms are also created using the SCM paradigm. To create jointed structures, rigid materials (carbon fiber reinforced composite prepregs) are cut as face sheets and polymers (typically polyimide) are used as the flexure. These are again bonded in a controlled cure cycle. This mechanism is shown in Figs. 2(d) and (e) and 5(a).

The actuator and transmission directly control the wing stroke. Wing rotation is developed passively with an additional flexure positioned between the output of the transmission and the wing. This flexure is parallel to the spanwise direction and includes joint-stops to avoid overrotation [see Fig. 5(c)]. Thus, this system has three degrees-of-freedom, only one of which is actuated [27] (as opposed to concurrent research on insect-inspired MAVs that attempt to concisely control each degree-of-freedom independently [10]).

C. Airfoils

The airfoils are designed to match the shape and size of the wings of Syrphid hoverflies. Insect wings have nontrivial anisotropic compliances [28], [29], but the airfoils used here are designed to remain rigid for all expected loading conditions. The airfoils are morphologically similar to insect wings; however, the "veins" consist of 30 μm thick ultrahigh modulus carbon fiber reinforced composite beams and the "membrane" is 1.5 μm thick polyester. The veins are arranged so that the wing is extremely rigid over the expected range of flight forces. To enable quasi-static passive wing rotation, the rotational inertia must be low such that the rotational resonant frequency is sufficiently high. Assuming underdamped second-order dynamics, an acceptable criterion for quasi-static rotation is that the first 3 dB point for rotation occurs above the flapping frequency. The 15 mm wing shown in Fig. 5(b) weighs 400 μg and remains undeformed during the entire stroke [see Fig. 7(a)]. These wings exhibit a remarkably high stiffness-to-weight ratio, which is a second example of the superiority of a micromechanical device over a biological system (due to significant differences between the material properties of chitin and carbon fiber).

IV. Results

Each of the components of the fly are assembled onto the airframe resulting in the structure shown in Fig. 1(b). To give an overall perspective, the finished robotic fly is compared to

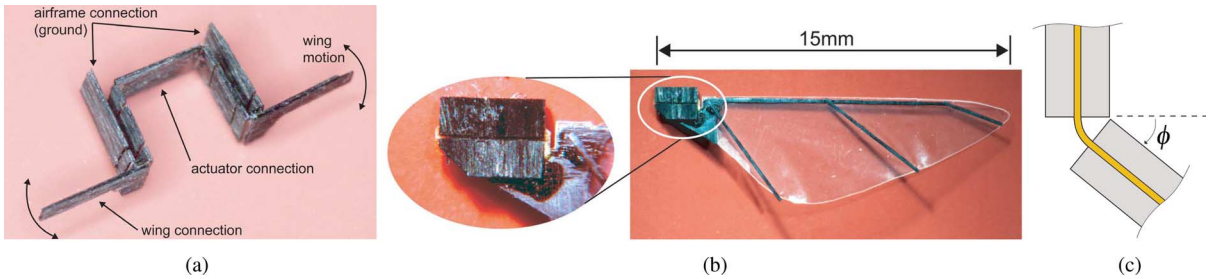

Fig. 5. Transmission (a) maps actuator motion to the wing stroke. Joint stops at the base of the airfoils (b, inset) limit the maximum angle of attack based upon the geometry of the hinge flexure (c).

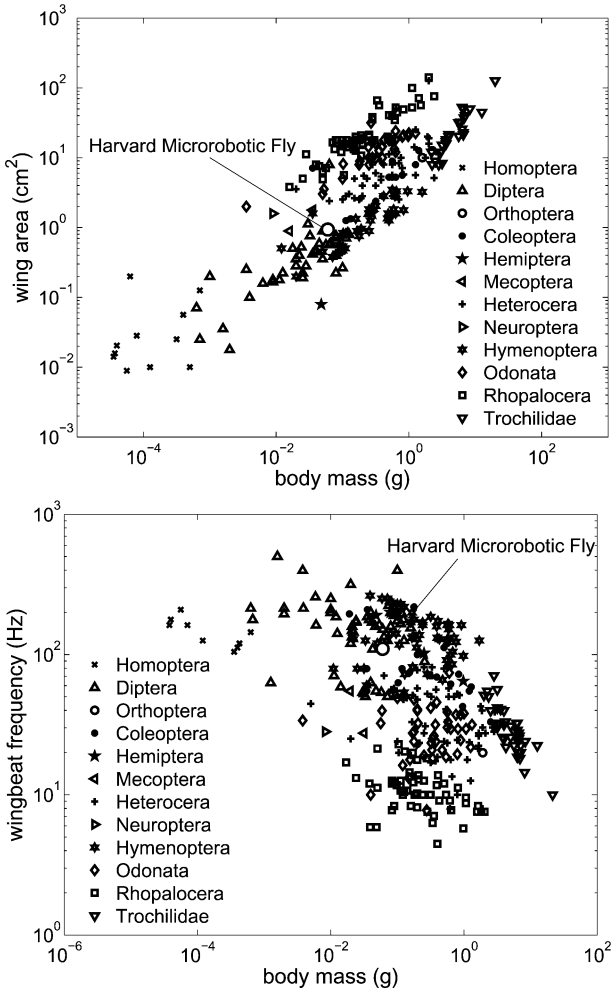

Fig. 6. Morphological and dynamic parameters of hover-capable biological examples as a function of body mass. It is clear that the device described here is consistent with biological trends (adapted form [17]).

TABLE I
MASS PROPERTIES FOR EACH COMPONENT OF THE MAV

component	mass (mg)
actuator	40
transmission	4
wings (×2)	≈0.5
airframe	11
misc. wiring, epoxy, etc.	5
total body	**60**

TABLE II
INTEGRATED MAV PERFORMANCE

total mass	60mg
wingspan	3cm
actuator PD	>150Wkg^{-1}
total PD	>100Wkg^{-1}
wing stroke	$> \pm 50°$
wing rotation	$\pm 50°$
wingbeat frequency	110Hz
peak wing velocity	> 6ms^{-1}
peak Re	≈1200

various hover-capable species in Fig. 6. The mass of each component in the integrated structure is given in Table I.

To isolate thrust from roll, pitch, and yaw moments, the robotic fly is fixed to taut guide wires that restrict the fly to purely vertical motion (guides are fabricated into the airframe). These wires are "training wheels" that will be incrementally removed in future research as attitude sensing and control are migrated onboard. The wings are driven open loop at the flapping resonance to maximize the stroke amplitude. For the MAV shown in Fig. 1, the resonant frequency is 110 Hz. So long as the rotational frequency is sufficiently higher than the flapping resonant frequency, the rotational component will operate quasi-statically. The natural frequency for wing rotation is calculated to be approximately 250 Hz based upon the flexural stiffness of the wing hinge and the rotational inertia of the wing [estimated from a computer-aided design (CAD) model]. Thus, the aerodynamic and inertial loads act to decrease the angle of attack, and the joint stops assure that the wings do not over-rotate. To visualize the wing motion, a high-speed video camera was used in two perspectives (lateral and anterior). Sequential frames from these videos are shown in Fig. 7. From the original high-speed video (≈20 frames/period), the wing kinematics are extracted (using custom Matlab software) and shown in Fig. 8. The trajectory is nearly identical to that of hovering Dipteran insects that lends credence to the use of passive rotation. However, the primary performance metric is the lift that is generated. This is assessed in two ways. First, the fly is fixed to a custom force sensor and the wings are driven open loop (maximum actuator drive field of 2 Vμm^{-1}). Lift measurement trials start by: 1) collecting the zero level of the sensor; 2) starting the wing from rest and allowing transients to decay (for 0.5 s at 10 kHz sample rate); and 3) collecting the force data (again for 0.5 s at 10 kHz corresponding to approximately 50 wing beats at 100 samples/period). Over ten trials, an average lift of 1.14 ± 0.23 mN is measured, corresponding to a thrust-to-weight ratio of

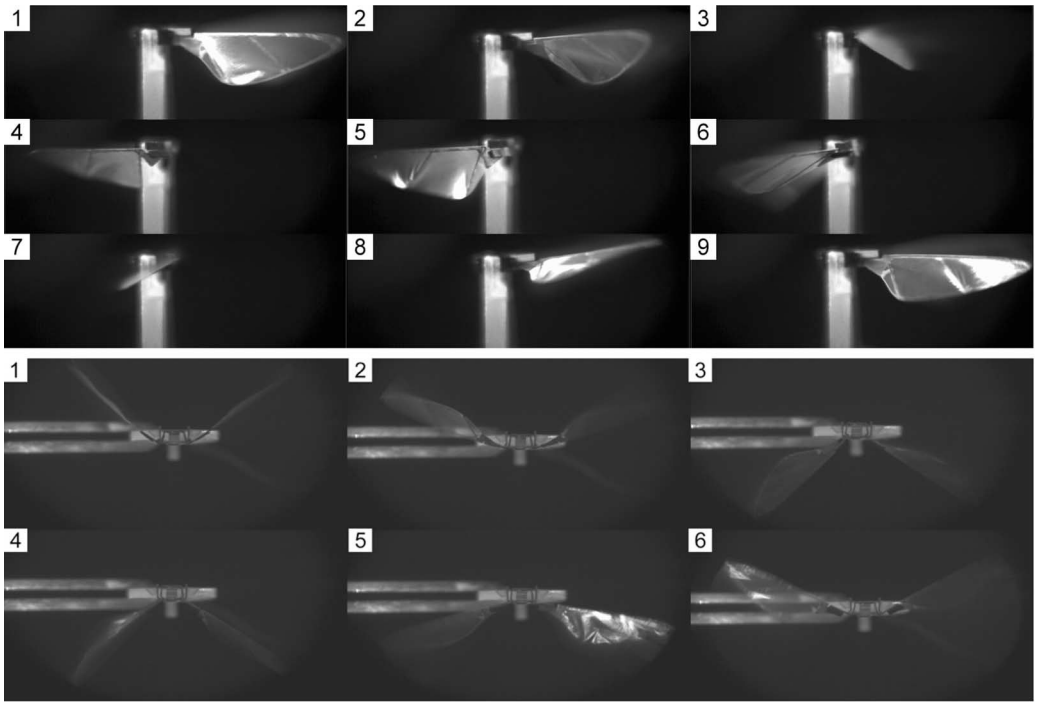

Fig. 7. (a) Wing motion as seen from a lateral perspective. (b) Anterior perspective. Frames are taken from a high-speed video sequence (left to right, top to bottom) of the wing moving at its flapping resonance. The lateral perspective is oriented to the midstroke: note that the symmetry and that the angle of attack at midstroke is approximately 40°.

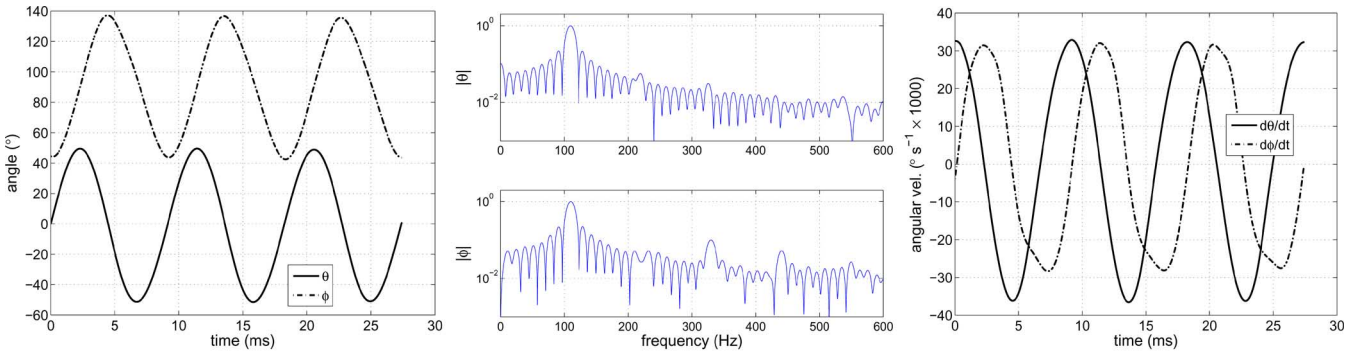

Fig. 8. (a) Wing trajectory extracted from anterior and lateral high-speed video sequences. (b) Flapping (θ) is mostly sinusoidal while rotation (ϕ) has significant components at other frequencies (most notably the third and fourth harmonics). (c) Angular velocities of the wing [as calculated from the angular positions in (a)].

approximately 2. Second, the integrated fly is aligned to the guide wires and allowed to freely move in the vertical direction. The wings are driven open loop and the fly ascends, as is shown in Fig. 9. This marks the first (tethered) liftoff of an insect-scale microrobot and validates the use of biological inspiration. Table II lists the key characteristics of the integrated fly.

V. Discussion

In summary, the performance of the Harvard Microrobotic Fly proves: 1) generating wing trajectories similar to Dipteran insects is possible with a robotic device and 2) propulsion generated by this microrobot is significant (compared to the body mass). However, these results do not show free flight, integrated sensing and control, or onboard power and electronics. Therefore, the Harvard Microrobotic Fly only represents a solution to the mechanical and aeromechanical components of an autonomous robotic insect. In order to create a fully autonomous flying microrobot, there are two additional research challenges that must be solved: 1) high-efficiency sensing, power conditioning, and control microelectronics and 2) a high energy density power source.

In previous work, a suite of biologically inspired sensors appropriate for attitude estimation and control has been developed [30]. This suite consists of sub-10 mg mechanoreceptive and photoreceptive sensors. Future development must evolve these into a monolithic solution for low-level (stabilization) sensors. Power and control electronics must also be created to drive the actuators. Both power and control architectures must be efficient, high bandwidth, and eventually occupy a very

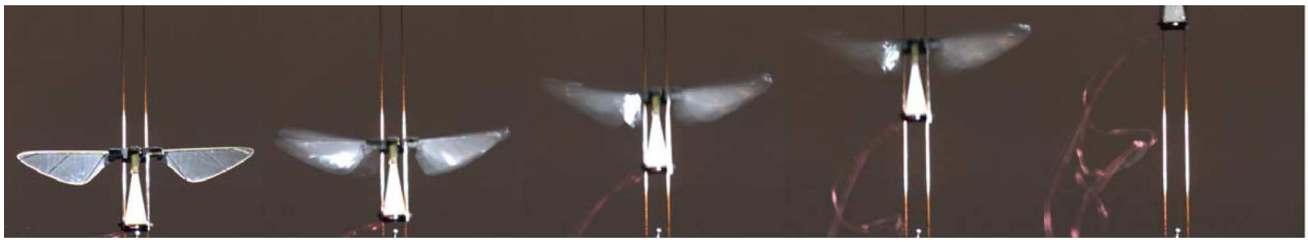

Fig. 9. First tethered flight of an at-scale robotic insect. From a video sequence spaced at approximately 100 ms intervals.

small volume of silicon. To compound these requirements, the piezoelectric actuators used in the Harvard Microrobotic Fly require high fields (approximately 2 Vμm^{-1}). Efficient, lightweight boost conversion [31], and drive electronics [32] for these actuators are ongoing research topics.

The final component necessary for a fully autonomous fly is a power source appropriate for both long duration flight and short energetic bursts. Based upon the electrical power requirements for the current fly, estimates of overall efficiency for the final version and the best available battery chemistry, it is estimated that fly-sized robots can operate for 5–10 min. However, this expected flight time is based upon the energy density of large-scale batteries. While there is no reason to expect that the chemistry should change with a decrease in physical dimensions, a decrease in size will result in a larger surface area to volume ratio, and thereby, require more packaging material for a given volume of battery. Furthermore, these numbers are for hovering in still air conditions. Gusts or air currents will require more power to remain stationary or follow a prescribed trajectory. The flight time will be incrementally increased by improvements in battery technology, increased propulsive efficiency, and the addition of energy harvesting devices (e.g. solar, vibrational, thermal, etc.).

It was noted that the maximum lift-to-weight ratio is approximately 2. However, this is only for the mechanical and aeromechanical structures. To enable the same specific thrust when power, electronics, and control are migrated onboard, we will need to further maximize the propulsive efficiency. For example, doubling the weight of the fly to 120 mg will require twice the current thrust to maintain a thrust-to-weight ratio of 2. This is a current focus that has begun with empirically verified wing modeling and optimization. It is useful at this point to investigate the mass distribution for the fully autonomous fly. This distribution is shown in Fig. 10. Note that in this distribution, the battery represents approximately 40% of the body mass. For terrestrial mobile robots, greater range can be achieved with a larger, higher capacity power source (within reasonable limits). However, for an aerial robot, this is not true since increased power supply mass will require larger lift forces to sustain flight. This increase in mechanical power translates into a corresponding increase in electrical power, and thus, increasing the battery mass has diminishing returns. The mechanical components in Fig. 10 do not require significant reduction from the current masses given in Table I. With regard to the electrical components, consider that a thinned silicon die with dimensions of 4 mm $\times$ 4 mm $\times$ 250 μm will have a mass just under 10 mg (with wiring). To put this in perspective, this chip would have

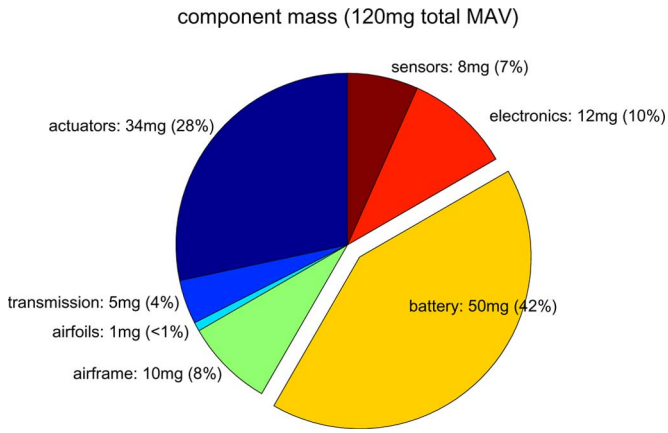

Fig. 10. Distribution of total MAV mass as predicted for the final, fully autonomous insect-scale MAV.

twice the area of a 8051 microcontroller and potentially 500 000 transistors. For perspective, a *Drosophila malanogaster* has approximately 300 000 neurons. The development of millimeter-scale ultralow energy controllers for autonomous microsystems has started for sensor network applications [33].

In earlier sections, there were two allusions to subsystems that outperform biological counterparts. This is by no means universal; there are countless aspects of flying insects that were heretofore unattainable with mechanical recreations. For example, evolution has done a phenomenal job with the integration of actuation, power, and control. However, due in part to recent advances in fabrication techniques (i.e., SCM), this gap is progressively narrowing.

Biological inspiration is ubiquitous in the mechanical subsystems that make up the Harvard Microrobotic Fly. Because of the relative ease of microfabrication allowed by SCM, these micromechanical devices can now be used in the opposite direction to gain insights into biological systems. For example, there are open questions pertaining to the scaling of biological airfoils and their compliances: do performance gains correspond to anisotropic compliances or are airfoil compliances simply due to biological material limitations? This may be a difficult question to answer with biological observation; but, by fabricating microrobotic airfoils with a large space of physical parameters, we can ascertain the role of compliance in lift generation, propulsive efficiency, stability, etc. This forms a sort of "closed-loop biological inspiration" that could be a valuable tool for biomechanics researchers.

REFERENCES

[1] C. P. Ellington, C. van der Berg, A. P. Willmott, and A. L. R. Thomas, "Leading-edge vortices in insect flight," *Nature*, vol. 384, pp. 626–630, Dec. 1996.

[2] S. Sunada and C. P. Ellington, "A new method for explaining the generation of aerodynamic forces in flapping flight," *Math. Methods Appl. Sci.*, vol. 24, pp. 1377–1386, 2001.

[3] M. H. Dickinson, F.-O. Lehmann, and S. P. Sane, "Wing rotation and the aerodynamic basis of insect flight," *Science*, vol. 284, pp. 1954–1960, Jun. 1999.

[4] M. H. Dickinson and K. G. Gotz, "The wake dynamics and flight forces of the fruitfly *Drosophila Melanogaster*," *J. Exp. Biol.*, vol. 199, pp. 2085–2104, 1999.

[5] S. N. Fry, R. Sayaman, and M. H. Dickinson, "The aerodynamics of free-flight maneuvers in *Drosophila*," *Science*, vol. 300, pp. 495–498, Apr. 2003.

[6] K. S. J. Pister, M. W. Judy, S. R. Burgett, and R. S. Fearing, "Microfabricated hinges," *J. Sens. Actuators A: Phys.*, vol. 33, pp. 249–256, 1992.

[7] W. S. N. Trimmer, "Microrobots and micromechanical systems," *J. Sens. Actuators*, vol. 19, pp. 267–287, 1989.

[8] R. J. Wood, S. Avadhanula, R. Sahai, E. Steltz, and R. S. Fearing, "Microrobot design using fiber reinforced composites," *J. Mech. Design*, to be published.

[9] S. Avadhanula, R. J. Wood, D. Campolo, and R. S. Fearing, "Dynamically tuned design of the MFI thorax," in *Proc. IEEE Int. Conf. Robot. Autom.*, Washington, DC, May 2002, vol. 1, pp. 52–59.

[10] S. Avadhanula, R. J. Wood, E. Steltz, J. Yan, and R. S. Fearing, "Lift force improvements for the micromechanical flying insect," in *Proc. IEEE/RSJ Int. Conf. Intell. Robots Syst.*, Las Vegas, Nevada, Oct. 2003, vol. 2, pp. 1350–1356.

[11] R. A. Brooks and A. M. Flynn, "Fast, cheap and out of control: A robot invasion of the solar system," *J. Brit. Interplanetary Soc.*, vol. 42, pp. 478–485, 1989.

[12] J. A. Miyan and A. W. Ewing, "Is the 'click' mechanism of dipteran flight an artefact of CCl_4 anaesthesia?," *J. Exp. Biol.*, vol. 116, pp. 313–322, 1985.

[13] J. A. Miyan and A. W. Ewing, "How Diptera move their wings: A re-examination of the wing base articulation and muscle systems concerned with flight," *Phil. Trans. R. Soc. Lond.*, vol. B311, pp. 271–302, 1985.

[14] H. K. Pfau, "Critical comments on a 'novel mechanical model of Dipteran flight' (Miyan & Ewing, 1985)," *J. Exp. Biol.*, vol. 128, pp. 463–468, 1987.

[15] J. A. Miyan and A. W. Ewing, "Further observations on Dipteran flight: Details of the mechanism," *J. Exp. Biol.*, vol. 136, pp. 229–241, 1988.

[16] M. H. Dickinson and M. S. Tu, "The function of dipteran flight muscle," *Comp. Biochem. Physiol.*, vol. 116A, pp. 223–238, 1997.

[17] R. Dudley, *The Biomechanics of Insect Flight: Form, Function and Evolution*. Princeton, NJ: Princeton Univ. Press, 1999.

[18] R. J. Wood, E. Steltz, and R. S. Fearing, "Optimal energy density piezoelectric bending actuators," *J. Sens. Actuators A: Phys.*, vol. 119, no. 2, pp. 476–488, 2005.

[19] M. Sun and J. H. Wu, "Aerodynamic force generation and power requirements in forward flight in a fruit fly with modeled wing motion," *J. Exp. Biol.*, vol. 206, pp. 3065–3083, 2003.

[20] M. H. Dickinson and J. R. B. Lighton, "Muscle efficiency and elastic storage in the flight motor of *Drosophila*," *Science*, vol. 268, pp. 87–90, Apr. 1995.

[21] F.-O. Lehmann and M. H. Dickinson, "The changes in power requirements and muscle efficiency during elevated force production in the fruit fly *Drosophila Melanogaster*," *J. Exp. Biol.*, vol. 200, pp. 1133–1143, 1997.

[22] M. S. Tu and T. L. Daniel, "Submaximal power output from the dorsolongitudinal flight muscles of the hawkmoth Manduca sexta," *J. Exp. Biol.*, vol. 207, pp. 4561–4662, 2004.

[23] E. Steltz and R. S. Fearing, "Dynamometer power output measurements of piezoelectric actuators," in *Proc. IEEE/RSJ Int. Conf. Intell. Robots Syst*, San Diego, CA, Oct. 2007, pp. 3980–3986.

[24] T. N. Pornsin-Shiriak, Y. C. Tai, H. Nassef, and C. M. Ho, "Titanium-alloy MEMS wing technology for a micro aerial vehicle application," *J. Sens. Actuators A: Phys.*, vol. 89, pp. 95–103, Mar. 2001.

[25] B. P. Trease, Y.-M. Moon, and S. Kota, "Design of large-displacement compliant joints," *J. Mech. Design*, vol. 127, pp. 788–798, Jul. 2005.

[26] S. Avadhanula and R. S. Fearing, "Flexure design rules for carbon fiber microrobotic mechanisms," in *Proc. IEEE Int. Conf. Robot. Autom.*, Barcelona, Spain, Apr. 2005, pp. 1579–1584.

[27] R. J. Wood, "Design, fabrication, and analysis, of a 3DOF, 3 cm flapping-wing MAV," in *Proc. IEEE/RSJ Int. Conf. Intell. Robots Syst.*, San Diego, CA, Oct. 2007, pp. 1576–1581.

[28] S. A. Combes and T. L. Daniel, "Flexural stiffness in insect wings I. Scaling and the influence of wing venation," *J. Exp. Biol.*, vol. 206, no. 17, pp. 2979–2987, 2003.

[29] S. A. Combes and T. L. Daniel, "Flexural stiffness in insect wings II. Spacial distribution and dynamic wing bending," *J. Exp. Biol.*, vol. 206, no. 17, pp. 2989–2997, 2003.

[30] W. C. Wu, L. Schenato, R. J. Wood, and R. S. Fearing, "Biomimetic sensor suite for flight control of a micromechanical flying insect: Design and experimental results," in *Proc. IEEE Int. Conf. Robot. Autom.*, Taipei, Taiwan, Sep. 2003, vol. 1, pp. 1146–1151.

[31] E. Steltz and R. S. Fearing, "Power electronics design choice for piezoelectric microrobots," in *Proc. IEEE/RSJ Int. Conf. Intell. Robots Syst*, Beijing, China, Oct. 2006, pp. 1322–1328.

[32] D. Campolo, M. Sitti, and R. S. Fearing, "Efficient charge recovery method for driving piezoelectric actuators with quasi-square waves," *IEEE Trans. Ultrason., Ferroelectr., Freq. Control*, vol. 50, no. 1, pp. 237–244, Mar. 2003.

[33] B. A. Warneke and K. S. J. Pister, "An ultra-low energy microcontroller for smart dust wireless sensor networks," presented at the Intl. Solid-State Circuits Conf. 2004 (ISSCC 2004), San Francisco, CA, Feb. 2004.

Robert J. Wood (M'01) received the M.S. and Ph.D. degrees in electrical engineering and computer science (EECS) from the University of California, Berkeley, in 2001 and 2004, respectively.

Since 2006, he has been with the School of Engineering and Applied Sciences, Harvard University, Cambridge, MA, as an Assistant Professor. His current research interests include mechatronics of microrobotic devices, particularly mobile microrobots for aerial, terrestrial, and aquatic environments, and underactuated processor-limited systems.